Optica Applicata, Vol. XXIX, No. 1–2, 1999

Notes of some properties of interferometric zone plate

EUGENIUSZ JAGOSZEWSKI

Institute of Physics, Wrocław University of Technology, Wybrzeże Wyspiańskiego 27, 50–370 Wrocław, Poland.

The difference between a conventional and an interferometric zone plate operation has been described. It is known that the interferometric zone plate as an axis point source hologram possesses only two foci, whereas the conventional one possesses a large number of focal lengths, both positive and negative. In this letter, some imaging properties of the interference zone plate are shown, and the zones of gradual transitions from minimum and maximum transmission are considered.

1. Introduction

The conventional zone plate (Fresnel zone plate) is a device on which there is a central spot surrounded by concentric annular zones, alternately opaque and transparent, with the radii of boundaries between the zones being proportional to the square roots of the natural numbers. Since the wave fronts from these transparent zones are in phase, it gives a high concetration of intensity at the focus, and it may be used as a lens to concentrate the energy in a light wave or to create images. The operation of zone plate is based on diffraction, whereas a lens operation is based on refraction, therefore the performance of a zone plate is different from the performance of a conventional lens.

In this paper, an interferometric zone plate [1], [2] generated by the interference of coherent plane and spherical waves, known as the Gabor zone plate is considered. When the interferometric zone plate is illuminated by a plane (or spherical) wave front of monochtomatic light, it produces only one virtual and one real point image, whereas the Fresnel zone plate produces an infinite number of point images. Indeed, the concept of the interferometric zone plate comes immediately from the Gabor's hologram theory.

2. Zones of an interferometric plate

The conventional zone plate is a kind of generalization of the pinhole camera and can overcome some of its disadvantages. This zone plate consists of a set of concentric circles with radii proportional to the square roots of whole numbers; when illuminated by a plane wave front of monochromatic light, the virtual and real images result at different points on the principal ray (optical axis). The focal length of such a zone plate is

$$f = \frac{r_n^2}{n\lambda} \quad (n = 1, 2, 3 \ldots), \tag{1}$$

where λ is the wavelength of the recording wave, and the fainter images correspond to the focal lengths: $\pm f/3$, $\pm f/5$, $\pm f/7$, ... Being still of weaker concentration at these distances, the Fresnel zone plates are not generally used in optical systems, because lenses that concentrate the light energy into a single focus give clearer images.

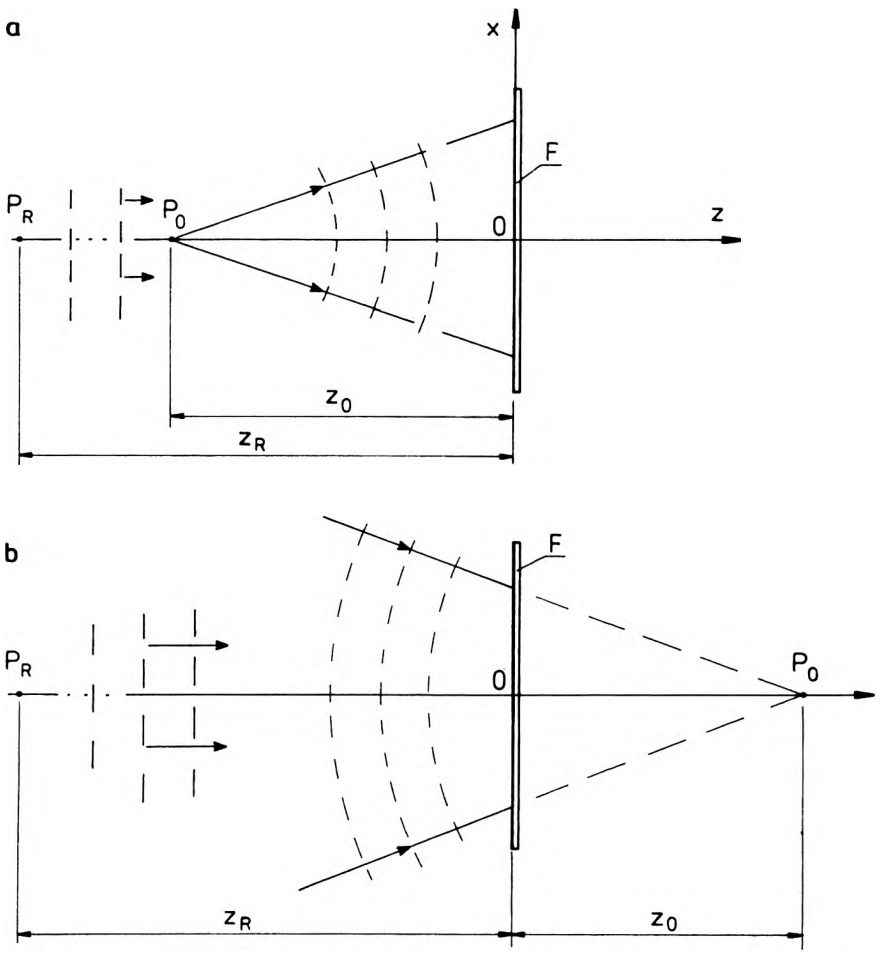

Fig. 1. Formation of an interferometric zone plate by a divergent (a) and a convergent (b) object wave front. P_O — object point source, P_R — reference point source inserted at infinity ($z_R \to \infty$).

Let us consider an on-axis hologram of a point object [3] that is produced at the photographic plate by recording the interference pattern of an object spherical and reference plane waves, both emitted from the axis point sources. Figure 1 illustrates this situation, where the recording plate is located in the x-y plane of the coordinate system. When the reference point source is inserted at the finite distance z_R from the photographic plate, the interference patterns are given by the intersection of the x-y plane with the two spherical surfaces of the recording wave fronts

$$[x^2+y^2+(z-z_O)^2]^{1/2}-[x^2+y^2+(z-z_R)^2]^{1/2}+(z_R-z_O)=n\lambda \tag{2}$$

where (x, y, z) are the coordinates of the intersection points of the surfaces in the photographic emulsion. The third term in the above equation is added to make the number n equal to zero at the origin of the coordinate system. Expanding as a power series in x and y by setting $z=0$, we obtain the first two terms in Eq. (2), approximately,

$$[x^2+y^2+(z-z_O)^2]^{1/2}=z_O+\frac{1}{2z_0}(x^2+y^2)-\frac{1}{8z_O^3}(x^2+y^2)^2,$$

$$[x^2+y^2+(z-z_R)^2]^{1/2}=z_R+\frac{1}{2z_R}(x^2+y^2)-\frac{1}{8z_R^3}(x^2+y^2)^2.$$

Therefore Eq. (2) takes the form

$$\left(\frac{1}{z_O}-\frac{1}{z_R}\right)\frac{(x^2+y^2)}{2}-\left(\frac{1}{z_O^3}-\frac{1}{z_R^3}\right)\frac{(x^2+y^2)^2}{8}=n\lambda, \tag{3}$$

or by substituting the following expressions:

$$z_R\to\infty,\quad z_O=f,\quad x^2+y^2=r_n^2,$$

we obtain for the paraxial region

$$f=\frac{r_n^2}{2n\lambda}. \tag{4}$$

The difference between Equations (1) and (4) lies in the fact that the amplitude transmittance of the zone plate described by Eq. (1) is rectangular and that of Eq. (4) is usually sinusoidal. In other words, the n-th number of zone Eq. (1) counts both opaque and transparent zones (or the inner and outer boundaries of the zones, separately for each zone), whereas in Eq. (4), n is the number of transparent zones. In this case, we can observe that the fact of one half of n in Eq. (1) being identical to n in Eq. (4), makes the intensity distribution changes just in each diffraction order. In place of the opaque and transparent zones of the conventional zone plate, we have gradual transitions from minimum to maximum transmission. The "rectangular" zone plate possesses a focusing property with a large number of focal lengths, both positive and negative, whereas the "sinusoidal" zone plate possesses only two foci.

An optical ray tracing for image formation by means of an interferometric zone plate is illustrated in Fig. 2. In this respect, the Rayleigh criterion for image formation can be used to determine the allowable number of transparent zones, *i.e.*, the error in optical path from the object to the sensibly perfect image should not exceed the value of $1/4\lambda$. The optical path from the object point P_O to its image at P_I can be written as

$$l=l_1+l_2=z_O+z_R+n\lambda \tag{5}$$

where n is the number of transparent zones. For a good image the optical path cannot vary more than the value determined by the Rayleigh criterion

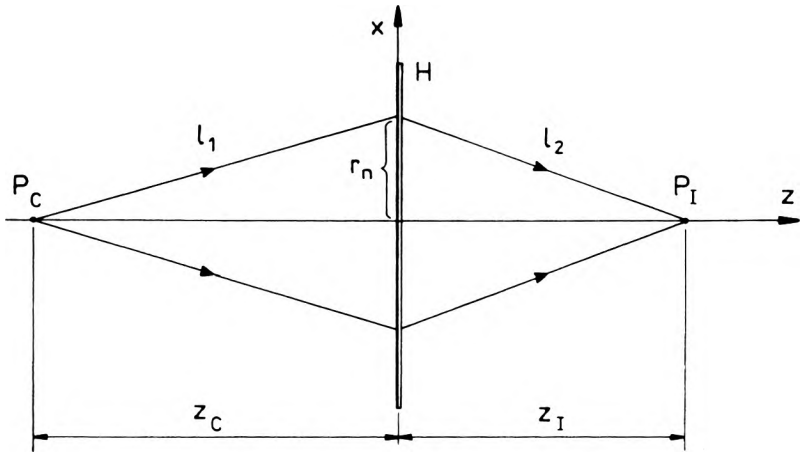

Fig. 2. Ray-tracing through an interferometric zone plate for image formation. P_C is an axial object point, and P_I is the image. H is its zone plate produced holographically.

$$l \leqslant \frac{1}{4}\lambda, \tag{6}$$

but $r_n^2 = (f+n\lambda)^2 - f^2 = 2n\lambda f + n^2\lambda^2$, and $\dfrac{1}{f} = \dfrac{1}{z_O} + \dfrac{1}{z_R}$.

On the other hand, by neglecting terms in higher powers of $n\lambda$, we have

$$l = \sqrt{z_O^2 + r_n^2} + \sqrt{z_R^2 + r_n^2} = z_O + z_R + n\lambda + \frac{n^2\lambda^2}{2f}\left[1 - \left(\frac{f}{z_O}\right)^3 - \left(\frac{f}{z_R}\right)^3\right].$$

Equating the right-hand side of the above equation with the appropriate expressions of Eq. (5) and the inequality (6), we obtain

$$\frac{1}{4} = \frac{n^2\lambda f^2}{2}\left(\frac{1}{f^3} - \frac{1}{z_O^3} - \frac{1}{z_R^3}\right). \tag{7}$$

The Rayleigh criterion for the image formation then leads to the following inequality:

$$\frac{1}{4} > \left|\frac{\lambda}{2f}n^2 - \frac{\lambda f^2}{2}n^2\left(\frac{1}{z_O^3} + \frac{1}{z_R^3}\right)\right| = \left|\frac{3}{2}\frac{\lambda f}{z_O z_R}n^2\right|,$$

$$n < \sqrt{\left|\frac{z_O z_R}{6f\lambda}\right|} = \frac{|z_O|}{\sqrt{6\lambda(z_O - f)}}. \tag{8}$$

The above equation shows that the allowable number of transparent zones for good image is proportional to the object distance in square root and, in particular, for the object at infinity when the object wave is normally incident on the zone plate, the number of zones is not limited.

3. Imaging and aberrations

Figure 1 illustrates the geometry of the interferometric zone plate recording process using a diverging (or converging) object wave and an on-axis collimated reference wave. The phase variation of the object wave at the zones plane is given by

$$\Phi(x, y) = \frac{2\pi}{\lambda}(\sqrt{f^2 + r_n^2} - f) \tag{9}$$

where the second term is included in the phase function to make $\Phi(x, y) = 0$ at $r_n = \sqrt{x^2 + y^2} = 0$. The circular spatial frequency of the zone plate at the distance r_n from the axis is determined as

$$\frac{d\Phi(r_n)}{dr_n} = \frac{2\pi r_n}{\lambda\sqrt{f^2 + r_n^2}}. \tag{10}$$

Hence the fringe spacing of the interferometric zone plate is

$$\Lambda = \lambda\sqrt{\left(\frac{f}{r_n}\right)^2 + 1}. \tag{11}$$

From Eq. (11) we can calculate the f-number of the zone plate

$$f\text{-number} = \frac{1}{2}\sqrt{\left(\frac{\Lambda}{\lambda}\right)^2 - 1}. \tag{12}$$

When equating the phase function (9) to $2\pi n$, we find the annular zones whose radii of constant phase are well known and expressed in the form

$$r_n = (2n\lambda f + n^2\lambda^2)^{1/2}.$$

But for $f \gg n\lambda$ the above expression is identical with the definition of the focal length of zone plate described by Eq. (4).

Let us consider an interferometric zone plate recorded as the on-axis point hologram illustrated in Fig. 1. The zone plate is illuminated by a spherical wave front emerging from a point source P_C to converge the reconstructed wave at the image point P_I. The relation between the point source and its image distances from the zone plate is described by the lens equation

$$\frac{1}{z_C} + \frac{1}{z_I} = \frac{2\lambda}{r_1^2} \tag{13}$$

where the image point P_I of the point source P_C is defined as the cross-point of the two rays that are diffracted at the points $P_1(x_1, y_1)$ and $P_2(x_2, y_2)$. The coordinates of the three points $P_1(x_1, y_1)$, $P(\bar{x}, \bar{y})$ as $P_2(x_2, y_2)$ indicated in Fig. 3 are connected with the radii of zones as follows:

$$r_{n-1} = \sqrt{(\bar{x} - z_C \tan\alpha_O)^2 + (\bar{y} - z_C \tan\alpha_O)^2},$$
$$r_n = \sqrt{\bar{x}^2 + \bar{y}^2},$$

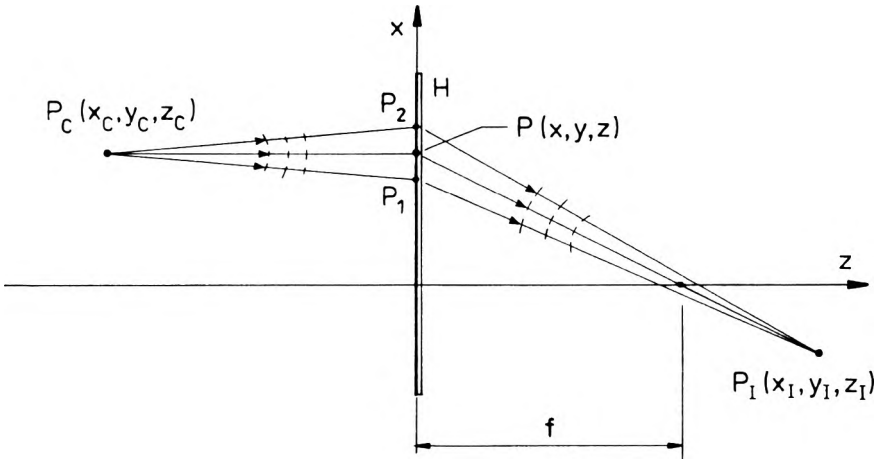

Fig. 3. Reconstruction of the interferometric zone plate by a coherent spherical wave that impinges normally on the zone plate at the r_n zone.

$$r_{n+1} = \sqrt{(\bar{x}+z_C\tan\alpha_O)^2+(\bar{y}+z_C\tan\alpha_O)^2}$$

where α_O is an object aperture angle. The diffraction angles at the three points P_1, P, P_2 in the figure plane are expressed, respectively, by the following relations

$$\alpha_1 = \sin^{-1}\left\{\sin\left[\tan^{-1}\sqrt{\frac{2(n-1)\lambda}{f}}\right]-\sin\left[\tan^{-1}\frac{\sqrt{2\lambda f}}{z_C}(\sqrt{n}-\sqrt{n-1})\right]\right\},$$

$$\alpha = \tan^{-1}\left(\sqrt{\frac{2n\lambda}{f}}\right),$$

$$\alpha_2 = \sin^{-1}\left\{\sin\left[\tan^{-1}\sqrt{\frac{2(n+1)\lambda}{f}}\right]+\sin\left[\tan^{-1}\frac{\sqrt{2\lambda f}}{z_C}(\sqrt{n+1}-\sqrt{n})\right]\right\}.$$

We then obtain the image distance as

$$z_I = \frac{\sqrt{8\lambda f}(\sqrt{n+1}-\sqrt{n})}{\tan\alpha_2-\tan\alpha_1}. \tag{14}$$

The variation of the image distance depends on the diffraction angles of the incident wave. But the f-number of the interferometric zone plate is determined by the image distance and the aperture diameter, therefore any imaging is here accomplished with errors.

The errors of an interferometric zone plate can be considered as the hologram aberrations, since this zone plate is made as a hologram of an axial point source. The hologram aberrations have been studied by MEIER [4] and CHAMPAGNE [5], and the aberrations of a zone plate by YOUNG [2], who studied the optical path difference expanded in a power series: OPD $= r_n^2/2f - r_n^4/8f^3 + \ldots$; here the second term determines the spherical aberration of a conventional zone plate illuminated

with parallel axial beam. The phase variation described by the function (9) can be applied to any area of the interferometric zone plate, for example, located about the point $P(\bar{x},\bar{y})$, as shown in Fig. 3. Expanding the phase function in a power series, we obtain

$$\Phi(x-\bar{x},y-\bar{y}) = \frac{2\pi}{\lambda}[\sqrt{f^2+(x-\bar{x})^2+(y-\bar{y})^2}-f]$$
$$= \frac{2\pi}{\lambda}\left\{\frac{1}{2f}[(x^2+\bar{x}^2)+(y^2+\bar{y}^2)]-\frac{1}{f}(\bar{x}x+\bar{y}y)\right\}$$
$$+\frac{2\pi}{\lambda}\left[\frac{1}{2f^3}[(x^2+y^2)(\bar{x}x+\bar{y}y)-(\bar{x}x+\bar{y}y)^2+(\bar{x}^2+\bar{y}^2)]\right.$$
$$\left.-\frac{1}{8f^3}[(x^2+y^2)+(\bar{x}^2+\bar{y}^2)]^2\right]+\ldots .$$

The first term of the above equation represents a spherical wave, and the second term changes the direction of the reconstructed wave. The remaining terms that are inversely proportional to f^3 determine the third order aberrations. In this way we determine the coma and astigmatism of the reconstructed off-axis wave front by the expressions: $(x^2+y^2)(\bar{x}x+\bar{y}y)$ and $(\bar{x}x+\bar{y}y)^2$, respectively.

In such an imaging, the astigmatism appeared to be the more serious aberration in the reconstructed wave front than coma.

References

[1] WALDMAN G. S., J. Opt. Soc. Am. **56** (1966), 215.
[2] YOUNG M., J. Opt. Soc. Am. **62** (1972), 972.
[3] COLLIER R., BURCKHARDT C. B., LIN L. H., *Optical Holography*, Academic Press, New York 1971.
[4] MEIER R. W., J. Opt. Soc. Am. **55** (1965), 987.
[5] CHAMPAGNE E. B., J. Opt. Soc. Am. **57** (1967), 51.

Received March 9, 1999